On Renewable Sensor Networks with Wireless Energy Transfer

Yi Shi[†]   Liguang Xie[†]   Y. Thomas Hou[†]   Hanif D. Sherali[‡]

[†] The Bradley Department of Electrical and Computer Engineering

[‡] The Grado Department of Industrial and Systems Engineering

Virginia Polytechnic Institute and State University, Blacksburg, VA, USA

Abstract—**Traditional wireless sensor networks are constrained by limited battery energy. Thus, finite network lifetime is widely regarded as a fundamental performance bottleneck. Recent breakthrough in the area of wireless energy transfer offers the potential of removing such performance bottleneck, i.e., allowing a sensor network remain operational forever. In this paper, we investigate the operation of a sensor network under this new enabling energy transfer technology. We consider the scenario of a mobile charging vehicle periodically traveling inside the sensor network and charging each sensor node's battery wirelessly. We introduce the concept of renewable energy cycle and offer both necessary and sufficient conditions. We study an optimization problem, with the objective of maximizing the ratio of the wireless charging vehicle (WCV)'s vacation time over the cycle time. For this problem, we prove that the optimal traveling path for the WCV is the shortest Hamiltonian cycle and provide a number of important properties. Subsequently, we develop a near-optimal solution and prove its performance guarantee.**

I. INTRODUCTION

Wireless sensor networks (WSNs) today are mainly powered by batteries. Due to limited energy storage capacity in a battery at each node, a WSN can only remain operational for a limited amount of time. To prolong its lifetime, there have been a flourish of research efforts in the last decade (see, e.g., [1], [2], [3], [4], [5]). Despite these intensive efforts, lifetime remains a performance bottleneck of a WSN and is perhaps one of the key factors that hinder its wide scale deployment.

Although energy-harvesting (or energy scavenging) techniques (see, e.g., [6], [7], [8, Chapter 9], [9], [10]) have been proposed to extract energy from the environment, their success remains limited in practice. This is because the proper operations of any energy-harvesting technique is highly dependent on the environment. Further, the size of an energy-harvesting device may pose a concern in deployment, particular when the size of such device is of much larger scale than the sensor node it is attempting to power.

Quite unexpectedly, the recent breakthrough in the area of *wireless energy transfer* technology developed by Kurs *et al.* [11] has opened up a revolutionary paradigm for sensor network lifetime. Basically, Kurs *et al.*'s work shows that by exploiting a novel technique called *magnetic resonance,* wireless energy transfer (i.e., the ability to transfer electric energy from one storage device to another *without any plugs or wires*) is both feasible and practical. In addition to wireless energy transfer, they have experimentally showed that the source energy storage device does not need to be in contact with the energy receiving device (e.g., a distance of 2 meters)

for efficient energy transfer. Further, such wireless energy transfer is immune to the neighboring environment and does not require line of sight between the energy charging and receiving nodes.

The impact of wireless energy transfer on WSNs or other energy-constrained wireless networks is immense. Instead of generating energy locally at a node (as in the case of energy harvesting), one can bring clean electric energy that are efficiently generated elsewhere to a sensor node periodically and charge its battery without the constraint of wires and plugs. As one can imagine, the applications of wireless energy transfer are numerous. For example, wireless energy transfer has already been applied to replenish battery energy in medical sensors and implantable devices [12] in healthcare industry.

Inspired by this new breakthrough energy transfer technology, this paper re-examines the network lifetime paradigm for a WSN. We envision employing a mobile vehicle carrying a battery charging station to periodically visit each sensor node and charge it wirelessly. This mobile wireless charging vehicle (WCV) can either be manned by human or be an autonomous vehicle. In this paper, we investigate the fundamental question of whether such new technology can remove the lifetime performance bottleneck from a battery-powered WSN, i.e., to have the WSN remain operational forever! The main contributions of this paper are the following.

- We introduce the concept of *renewable energy cycle* where the remaining energy level in a sensor node's battery exhibit some periodicity over a time cycle. We offer both necessary and sufficient conditions for renewable energy cycle and show that feasible solutions satisfying these conditions can offer renewable energy cycles and thus, unlimited sensor network lifetime.
- We formulate an optimization problem, with the objective of maximizing the ratio of the WCV's vacation time (time spent at its home service station) over the cycle time. For this problem, we prove that the optimal traveling path for the WCV in each renewable cycle is the shortest Hamiltonian cycle. We also derive several interesting properties associated with an optimal solution, such as the optimal objective being independent of traveling direction on the shortest Hamiltonian cycle and the existence of a bottleneck node in the network.
- Under the optimal traveling path, our optimization problem now only need to consider flow routing and charging time for each sensor node. By showing that traditional minimum energy routing is non-optimal, we formulate a joint optimization problem for flow routing and charging

time for each sensor node. The problem is shown to be a nonlinear optimization problem and is NP-hard in general.

- For our optimization problem, we develop a provable near-optimal solution for any desired level of accuracy.

The remainder of this paper is organized as follows. In Section II, we review recent advances in wireless energy transfer technology. In Section III, we describe the scope of our problem for a renewable sensor network. Section IV introduces the concept of renewable energy cycle and presents some interesting properties. Section V shows that an optimal traveling path should be along the shortest Hamiltonian path. In Section VI, we present our problem formulation and a near-optimal solution. Section VII shows how to construct the initial transient cycle after which a renewable cycle can start. In Section VIII, we present numerical results to demonstrate the properties of a renewable wireless sensor network under our solution. Section IX concludes this paper.

II. WIRELESS ENERGY TRANSFER: A PRIMER

Efforts of transferring power wirelessly can be dated back to the early 1900s (long before wired electric power grid) when Nikola Tesla experimented with large scale wireless power distribution [13]. Due to its large electric fields, which is undesirable for efficient energy transfer, Tesla's invention was never put into practice use.

Since then, there was hardly any progress in wireless energy transfer for many decades. In early 1990s, the critical need of wireless power transfer re-emerged due to wide spread use of portable electronic devices (see, e.g., [14]). The most well known example is electric toothbrush. However, due to stringent requirements such as close in contact, accurate alignment in charging direction, and uninterrupted line of sight, most of the wireless power transfer technologies (based on radiative transfer) at the time only found limited applications.

The foundation of our work in this paper is based on a recent breakthrough technology by Kurs *et al.* [11], which was published in *Science* in 2007 and has since caught worldwide attention. In [11], Kurs *et al.* experimentally demonstrated efficient non-radiative energy transfer is not only possible, but also practical. They used two magnetic resonant objects of the same resonant frequency to exchange energy efficiently, while dissipating relatively little energy in extraneous off-resonant objects. They showed that efficient power transfer implemented in this way can be nearly omnidirectional, irrespective of the environment and even without line of sight. A highlight of their experiment was to fully powering a 60-W light bulb from a distance of 2 meters away.

With the recent establishment of Wireless Power Consortium [15] to set the international standard for interoperable wireless charging, it is expected that wireless energy transfer will revolutionize how energy is exchanged in the near future.

III. PROBLEM DESCRIPTION

We consider a set of sensor nodes $\mathcal{N}$ distributed over a two-dimensional area. Each sensor node has a battery capacity of $E_{\max}$ and is fully charged initially. Also, denote $E_{\min}$ the minimum energy at a sensor node battery (for it to be operational). Each sensor node i generates sensing data with a rate of R_i (in b/s), $i \in \mathcal{N}$. Within the sensor network, there is a fixed base station (B), which is the sink node for all data generated by the sensor nodes. Multi-hop data routing can be employed for forwarding data by the sensor nodes. Denote f_{ij} the flow rate from sensor node i to sensor node j and f_{iB} the flow rate from sensor node i to the base station B, respectively. Then we have the following flow balance constraint at each sensor node i.

$$\sum_{k \in \mathcal{N}}^{k \neq i} f_{ki} + R_i = \sum_{j \in \mathcal{N}}^{j \neq i} f_{ij} + f_{iB} \quad (i \in \mathcal{N}). \quad (1)$$

Each sensor node consumes energy for data transmission and reception. Denote p_i the energy consumption rate at sensor node $i \in \mathcal{N}$. In this paper, we use the following energy consumption model [4].

$$p_i = \rho \sum_{k \in \mathcal{N}}^{k \neq i} f_{ki} + \sum_{j \in \mathcal{N}}^{j \neq i} C_{ij} f_{ij} + C_{iB} f_{iB} \quad (i \in \mathcal{N}) , \quad (2)$$

where ρ is the rate of energy consumption for receiving a unit of data rate, C_{ij} (or C_{iB}) is the rate of energy consumption for transmitting a unit of data rate from node i to node j (or the base station B). Further, $C_{ij} = \beta_1 + \beta_2 D_{ij}^{\alpha}$, where D_{ij} is the distance between nodes i and j, β_1 is a distance-independent constant term, β_2 is a coefficient of the distance-dependent term and α is the path loss index. In the model, $\rho \sum_{k \in \mathcal{N}}^{k \neq i} f_{ki}$ is the energy consumption rate for reception, and $\sum_{j \in \mathcal{N}}^{j \neq i} C_{ij} f_{ij} + C_{iB} f_{iB}$ is the energy consumption rate for transmission.

To recharge the battery at each sensor node, a mobile wireless charging vehicle (WCV) is employed in the network. The WCV starts from a service station (S), and the traveling speed of the WCV is V (in m/s). When it arrives at a sensor node, say i, it will spend a time of τ_i to charge the sensor node's battery wirelessly via non-radiative energy transfer [11]. Denote U the energy transfer rate of the WCV. After τ_i, the WCV leaves node i and travels to the next node. We assume that the WCV has enough energy to charge all sensor nodes in the network.

After the WCV visits all the sensor nodes in the network, it will return to its service station to be serviced (e.g., replacing or recharging its battery) and get ready for the next trip. We call this resting period *vacation time*, denoted as τ_{vac}. After this vacation, the WCV will go out for its next trip.

Denote the time for a trip cycle of the WCV as τ. A number of questions can be raised for such a re-chargeable sensor network. First and foremost, one would inquire whether it is possible to have each sensor node never run out of its energy? If this is possible, then the sensor network will have unlimited lifetime and will never cease to be operational. Second, if the answer to the first question is positive, then is there any optimal plan (including traveling path, stop schedule) such that some useful objective can be maximized or minimized? For example, in this paper, we would like to maximize the percentage of time in a cycle that the WCV can take vacation (i.e., $\frac{\tau_{\mathrm{vac}}}{\tau}$), or equivalently, to minimize the percentage of time that the WCV is out in the field.

IV. RENEWABLE CYCLE CONSTRUCTION

In this section, we focus on the renewable cycle construction. We assume the WCV starts from the service station,
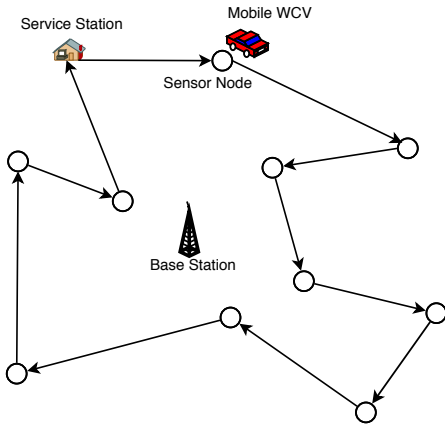
Fig. 1.   A wireless sensor network with a wireless charging vehicle (WCV).

Fig. 2.   The energy level of a sensor node i during the first two renewable cycles (partially re-charged v.s. fully re-charged).

visits each sensor node once in a cycle and ends at the service station (see Fig. 1). Further, we assume data flow routing in the network is invariant with time, with both routing and flow rates being part of our optimization problem.

The middle sawtooth graph (in dashed line) in Fig. 2 shows the energy level of a sensor node i during the first two renewable cycles. Note that there is an initialization cycle (marked in grey area) before the first renewable cycle. That initialization cycle will be constructed in Section VII once we have an optimal solution to the renewable cycles.

Denote $P = (\pi_0, \pi_1, \ldots, \pi_N, \pi_0)$ the physical path traversed by the WCV over a trip cycle, which starts from and ends at the service station (i.e., $\pi_0 = S$) and the ith node traversed by the WCV along path P is π_i, $i \in \mathcal{N}$. Denote $D_{\pi_0 \pi_1}$ the distance between the service station and the first sensor node visited along P and $D_{\pi_k \pi_{k+1}}$ the distance between the kth and $(k+1)$th sensor nodes, respectively. Denote a_i the arrival time of the WCV at sensor node i in the first renewable energy cycle. We have

$$a_{\pi_i} = \tau + \sum_{k=0}^{i-1} \frac{D_{\pi_k \pi_{k+1}}}{V} + \sum_{k=1}^{i-1} \tau_k . \qquad (3)$$

Denote D_P the physical distance of path P and $\tau_P = D_P/V$ the time used for traveling over distance D_P. Recall that τ_{vac} is the vacation time the WCV spends at its service station. Then the cycle time τ can be written as

$$\tau = \tau_P + \tau_{\mathrm{vac}} + \sum_{i \in \mathcal{N}} \tau_i . \qquad (4)$$

We formally define a renewable energy cycle as follows.

Definition 1: The energy level of a sensor node $i \in \mathcal{N}$ exhibits a renewable energy cycle if it meets the following two requirements: (i) it starts and ends with the same energy level over a period of τ; and (ii) it never falls below $E_{\min}$.

During a renewable cycle, the amount of charged energy at a sensor node i during τ_i must be equal to the amount of energy consumed in the cycle (so as to ensure the first requirement in Definition 1). That is,

$$\tau \cdot p_i = \tau_i \cdot U \quad (i \in \mathcal{N}) . \qquad (5)$$

Note that when the WCV visits a node i at time a_i during a renewable energy cycle, it does not have to re-charge the sensor node's battery to $E_{\max}$. This is illustrated in Fig. 2,
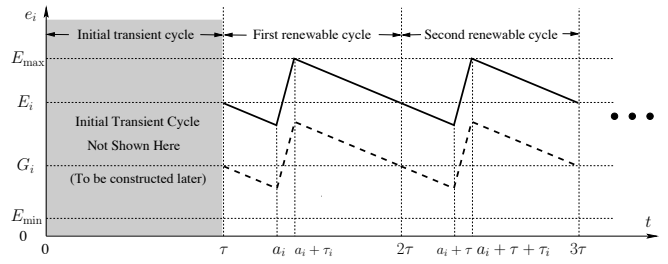
where G_i denotes the starting energy of sensor node i in a renewable cycle and $g_i(t)$ the energy level at time t (dashed sawtooth graph). During a cycle $[\tau, 2\tau]$, we see that the energy level has only two slopes: (i) a slope of $-p_i$ when the WCV is not at this node (i.e., non-charging period), and (ii) a slope of $(U - p_i)$ when the WCV is charging this node at a rate of U (i.e., charging period). It is clear that $g_i(a_i) \leq g_i(t) \leq g_i(a_i + \tau_i)$, i.e., node i's energy level is lowest at time a_i and is highest at time $a_i + \tau_i$.

Also show in Fig. 2 is another renewable energy cycle (marked in solid sawtooth graph) where the battery energy is charged to $E_{\max}$ during a WCV's visit. For this energy curve, denote E_i the starting energy of node i in a renewable cycle and $e_i(t)$ as the energy level at time t, respectively. Let $\varphi^*_{\mathrm{Full}}$ be an optimal solution with fully re-charged battery in each cycle. Let φ^* be an optimal solution that maximizes the ratio of the WCV's vacation time over the cycle time, where there is no requirement on whether or not a node's battery is fully re-charged. Naturally, the optimal objective obtained by $\varphi^*_{\mathrm{Full}}$ is no more than the optimal objective obtained by φ^* due to the additional requirement (battery is fully re-charged) in $\varphi^*_{\mathrm{Full}}$. Surprisingly, the following lemma shows that $\varphi^*_{\mathrm{Full}}$ is equally good as φ^* in terms of maximizing the ratio of the WCV's vacation time over the cycle time. Thus, for our optimization problem, it is sufficient to consider a solution with fully re-charged battery. We omit the proof here due to space limit and refer readers to [16] for details.

Lemma 1: Solution $\varphi^*_{\mathrm{Full}}$ can achieve the same maximum ratio of vacation time to the cycle time as that by solution φ^*.

Based on Lemma 1, we will only consider renewable cycle where each node is fully re-charged when it is visited by the WCV. Since the energy level at node i is lowest at time a_i, to ensure the second requirement in Definition 1, we must have $e_i(a_i) = E_i - (a_i - \tau)p_i \geq E_{\min}$. Since for a renewable cycle,

$$\begin{aligned} E_i = e_i(2\tau) &= e_i(a_i + \tau_i) - (2\tau - a_i - \tau_i)p_i \\ &= E_{\max} - (2\tau - a_i - \tau_i)p_i . \end{aligned} \qquad (6)$$

Then we have $e_i(a_i) = E_{\max} - (2\tau - a_i - \tau_i)p_i - (a_i - \tau)p_i = E_{\max} - (\tau - \tau_i)p_i$. Therefore,

$$E_{\max} - (\tau - \tau_i) \cdot p_i \geq E_{\min} \quad (i \in \mathcal{N}) . \qquad (7)$$

For a renewable energy cycle, we have the following lemma.

Lemma 2: A cycle is a renewable energy cycle if and only if constraints (4), (5) and (7) are met for each sensor node $i \in \mathcal{N}$.

The proof of Lemma 2 is omitted to conserve space. We refer readers to [16] for details.

The following property shows that in an optimal solution, there exists at least one "bottleneck" node in the network, where the energy level at this node drops exactly to $E_{\min}$ when the WCV arrives and starts to charge this node's battery.

Property 1: In an optimal solution, there exists at least one node in the network with its battery energy dropping to $E_{\min}$ when the WCV arrives at this node.

A proof of this property is given in [16].

V. Optimal Traveling Path

In this section, we show that the WCV must move along the shortest Hamiltonian cycle in an optimal solution, which is formally stated in the following theorem.

Theorem 1: In an optimal solution with the maximal $\frac{\tau_{\mathrm{vac}}}{\tau}$, the WCV must move along the shortest Hamiltonian cycle that crosses all the sensor nodes and the service station.

Theorem 1 can be proved by contradiction. That is, if there is an optimal solution φ^*, where the WCV does not move along the shortest Hamiltonian cycle, then we can construct a new solution $\hat{\varphi}$ with the WCV moving along the shortest Hamiltonian cycle and with an improved objective. This solution $\hat{\varphi}$ is constructed by changing the traveling path in φ^* by the shortest Hamiltonian cycle (thus the traveling time is decreased and the vacation time can be increased) and keeping all other variables (for flow rates, charging time, and cycle time) unchanged. The details of this proof are given in [16].

Theorem 1 gives us an interesting result that the WCV should move along the shortest Hamiltonian cycle, which can be obtained by solving the well known Traveling Salesman Problem (TSP) (see, e.g., [17], [18]). Denote D_{TSP} as the total path distance in the shortest Hamiltonian cycle and $\tau_{\mathrm{TSP}} = D_{\mathrm{TSP}}/V$. Then with the optimal traveling path, (4) becomes

$$\tau_{\mathrm{TSP}} + \tau_{\mathrm{vac}} + \sum_{i \in \mathcal{N}} \tau_i = \tau . \qquad (8)$$

We note that the shortest Hamiltonian cycle may not be unique. Since any shortest Hamiltonian cycle has equivalent total path distance and traveling time τ_{TSP}, the selection of a particular shortest Hamiltonian cycle does not affect constraint (8), and yields the same optimal objective. This insight is formally stated in the following corollary.

Corollary 1.1: Any shortest Hamiltonian cycle can achieve the same optimal objective.

We also note that to travel the shortest Hamiltonian cycle, there are two (opposite) outgoing directions for the WCV to start from its home service station. Since the proof of Theorem 1 is independent of the starting direction for the WCV, either direction will yield some optimal solution with the same objective value, although some variables in each optimal solution will have different values. We have the following corollary.

Corollary 1.2: To complete the shortest Hamiltonian cycle, there are two opposite directions that the WCV can follow, both of which can achieve the same optimal objective. In the two

optimal solutions corresponding to the two opposite directions, the values of $f_{ij}, f_{iB}, \tau, \tau_i, \tau_{\mathrm{TSP}}, \tau_{\mathrm{vac}}, p_i$ are identical, while the values of a_i (by (3)) and E_i (by (6)) are different due to difference in their respective renewable cycles, where $i, j \in \mathcal{N}$, $i \neq j$.

VI. Problem Formulation and Solution

A. Mathematical Formulation

Summarizing the objective and all the constraints in Sections III, IV and V, our problem can be formulated as follows.

OPT

$$\max \qquad \frac{\tau_{\mathrm{vac}}}{\tau}$$

$$s.t. \qquad (1), (2), (5), (7), (8)$$

$$f_{ij}, f_{iB}, \tau_i, \tau, \tau_{\mathrm{vac}}, p_i \geq 0 \quad (i, j \in \mathcal{N}, i \neq j)$$

In this problem, flow rates f_{ij} and f_{iB}, time intervals τ, τ_i, and τ_{vac}, and power consumption p_i are optimization variables; R_i, C, C_{ij}, C_{iB}, U, $E_{\max}$, $E_{\min}$, and τ_{TSP} are constants. This problem has both nonlinear objective ($\frac{\tau_{\mathrm{vac}}}{\tau}$) and nonlinear terms ($\tau p_i$ and $\tau_i p_i$) in constraints (5) and (7).

We note that in the above formulation, only the constant τ_{TSP} is related to the shortest Hamiltonian cycle. Since this value does not depend on the traveling direction along the Hamiltonian cycle, an optimal solution of problem OPT can work with either direction and yields one renewable cycle for each direction.

B. Reformulation

We first use change-of-variable technique to simplify the formulation. For the nonlinear objective $\frac{\tau_{\mathrm{vac}}}{\tau}$, we define

$$\eta_{\mathrm{vac}} = \frac{\tau_{\mathrm{vac}}}{\tau} . \qquad (9)$$

For (8), we divide both sides by τ and have $\tau_{\mathrm{TSP}} \cdot \frac{1}{\tau} + \eta_{\mathrm{vac}} + \sum_{i \in \mathcal{N}} \frac{\tau_i}{\tau} = 1$. To remove the nonlinear terms $\frac{1}{\tau}$ and $\frac{\tau_i}{\tau}$ in the above equation, we define

$$\eta_i = \frac{\tau_i}{\tau} \quad (i \in \mathcal{N}) , \qquad (10)$$

$$h = \frac{1}{\tau} . \qquad (11)$$

Then (8) is reformulated as $\tau_{\mathrm{TSP}} \cdot h + \eta_{\mathrm{vac}} + \sum_{i \in \mathcal{N}} \eta_i = 1$, or equivalently,

$$h = \frac{1 - \sum_{i \in \mathcal{N}} \eta_i - \eta_{\mathrm{vac}}}{\tau_{\mathrm{TSP}}} . \qquad (12)$$

Similarly, (5) and (7) can be reformulated (by dividing both sides by τ) as

$$p_i = U \cdot \eta_i \qquad (i \in \mathcal{N}) , \qquad (13)$$

$$(1 - \eta_i) \cdot p_i \leq (E_{\max} - E_{\min}) \cdot h \quad (i \in \mathcal{N}) . \qquad (14)$$

By (12) and (13), constraint (14) can be rewritten as $(1 - \eta_i) \cdot U\eta_i \leq (E_{\max} - E_{\min}) \frac{1 - \sum_{k \in \mathcal{N}} \eta_k - \eta_{\mathrm{vac}}}{\tau_{\mathrm{TSP}}}$, or

$$\eta_{\mathrm{vac}} \leq 1 - \sum_{k \in \mathcal{N}} \eta_k - \frac{U \cdot \tau_{\mathrm{TSP}}}{E_{\max} - E_{\min}} \cdot \eta_i \cdot (1 - \eta_i) \quad (i \in \mathcal{N}) .$$

By (13), constraint (2) can be rewritten as

$$C \sum_{k \in \mathcal{N}}^{k \neq i} f_{ki} + \sum_{j \in \mathcal{N}}^{j \neq i} C_{ij} f_{ij} + C_{iB} f_{iB} - U\eta_i = 0 \quad (i \in \mathcal{N}) .$$

Now the problem OPT is reformulated as follows.

OPT-R

$$\max \qquad \eta_{\text{vac}}$$

$$s.t. \quad \sum_{j \in \mathcal{N}}^{j \neq i} f_{ij} + f_{iB} - \sum_{k \in \mathcal{N}}^{k \neq i} f_{ki} = R_i \quad (i \in \mathcal{N}) \quad (15)$$

$$C \sum_{k \in \mathcal{N}}^{k \neq i} f_{ki} + \sum_{j \in \mathcal{N}}^{j \neq i} C_{ij} f_{ij} + C_{iB} f_{iB} - U\eta_i = 0$$
$$(i \in \mathcal{N}) \quad (16)$$

$$\eta_{\text{vac}} \leq 1 - \sum_{k \in \mathcal{N}} \eta_k - \frac{U \cdot \tau_{\text{TSP}}}{E_{\max} - E_{\min}} \cdot \eta_i \cdot (1 - \eta_i)$$
$$(i \in \mathcal{N}) \quad (17)$$

$$f_{ij}, f_{iB} \geq 0, 0 \leq \eta_i, \eta_{\text{vac}} \leq 1 \qquad (i, j \in \mathcal{N}, i \neq j)$$

In this problem, f_{ij}, f_{iB}, η_i, and η_{vac} are optimization variables; R_i, C, C_{ij}, C_{iB}, U, $E_{\max}$, $E_{\min}$ and τ_{TSP} are constants. The following algorithm shows how to obtain a solution to problem OPT once we obtain a solution to problem OPT-R.

Algorithm 1: Once we solve problem OPT-R, we can obtain the solution to problem OPT (i.e., calculate the values for τ, τ_i, τ_{vac}, and p_i) as follows: h by (12), τ by (11), τ_i by (10), τ_{vac} by (9), and p_i by (13).

After reformulation, the objective function and the constraints become linear except (17), where we have a second order η_i^2 term, with $0 \leq \eta_i \leq 1$. In the next section, we present an efficient technique to approximate this second order nonlinear terms. Subsequently, we develop an efficient near-optimal solution to our optimization problem.

Remark 1: In our optimization problem, data routing and charging time are closely coupled. One may want to decouple routing from the charging problem and opt certain energy efficient routing, e.g., the minimum energy routing.[1] However, minimum energy routing cannot guarantee optimality. This is because, to maximize η_{vac}, by (17), we need to minimize $\max_{i \in \mathcal{N}} \{\sum_{k \in \mathcal{N}} \eta_k + \frac{U \cdot \tau_{\text{TSP}}}{E_{\max} - E_{\min}} \cdot \eta_i \cdot (1 - \eta_i)\}$, i.e., minimize $\{\sum_{k \in \mathcal{N}} \eta_k + \max_{i \in \mathcal{N}} \{\frac{U \cdot \tau_{\text{TSP}}}{E_{\max} - E_{\min}} \cdot \eta_i \cdot (1 - \eta_i)\}\}$. But under minimum energy routing, we can only guarantee that $\sum_{i \in \mathcal{N}} (C \sum_{k \in \mathcal{N}}^{k \neq i} f_{ki} + \sum_{j \in \mathcal{N}}^{j \neq i} C_{ij} f_{ij} + C_{iB} f_{iB})$ is minimized. By the relationship in (16), minimizing $\sum_{i \in \mathcal{N}} (C \sum_{k \in \mathcal{N}}^{k \neq i} f_{ki} + \sum_{j \in \mathcal{N}}^{j \neq i} C_{ij} f_{ij} + C_{iB} f_{iB})$ is equivalent to minimizing $\sum_{i \in \mathcal{N}} \eta_i$, which is only part of $\sum_{k \in \mathcal{N}} \eta_k + \max_{i \in \mathcal{N}} \{\frac{U \cdot \tau_{\text{TSP}}}{E_{\max} - E_{\min}} \cdot \eta_i \cdot (1 - \eta_i)\}$. Therefore, minimum energy routing cannot guarantee optimality of our problem. This insight will be confirmed by our numerical results in Section VIII. $\square$

C. A Near-Optimal Solution

Roadmap. Our roadmap to solve problem OPT is as follows. First, we employ a piecewise linear approximation for the quadratic terms (η_i^2) in problem OPT-R. This approximation relaxes the corresponding nonlinear constraints into linear

---

[1]Here, minimum energy routing is defined as using the least energy route to transport data from its source to destination.
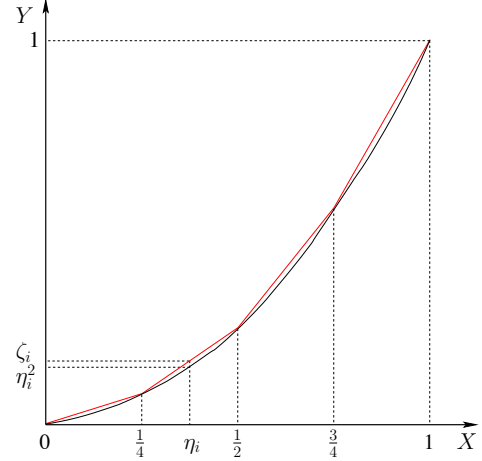
Fig. 3. An illustration of piecewise linear approximation (with $m = 4$) for the curve (η_i, η_i^2), $0 \leq \eta_i \leq 1$.

constraints, which allows for the problem to be solved by a solver such as CPLEX [19]. Based on the solution from CPLEX, we construct a feasible solution to problem OPT. In Section VI-D, we prove the near-optimality of this feasible solution.

Piecewise Linear Approximation for η_i^2. Note that the only nonlinear terms in the formulation are η_i^2, $i \in \mathcal{N}$. Further, η_i lies in the interval $[0, 1]$, which is small. This motivates us to employ a piecewise linear approximation for the quadratic terms η_i^2.

The key idea is to use m piecewise linear segments to approximate the quadratic curve (see Fig. 3). That is, for curve (η_i, η_i^2), $0 \leq \eta_i \leq 1$, we construct a piecewise linear approximation (η_i, ζ_i) by connecting points $(\frac{k}{m}, \frac{k^2}{m^2})$, $k = 0, 1, \ldots, m$. The setting of m will determine the level of accuracy and will be studied in Section VI-D.

We now represent the piecewise linear curve (η_i, ζ_i) for $0 \leq \eta_i \leq 1$ mathematically. For $k = 0, 1, \ldots, m$, any point (η_i, ζ_i) on the piecewise linear curve within the kth segment (i.e., lying within two end points $(\frac{k-1}{m}, \frac{(k-1)^2}{m^2})$ and $(\frac{k}{m}, \frac{k^2}{m^2})$) can be represented by

$$\eta_i = \lambda_{i,k-1} \cdot \frac{k-1}{m} + \lambda_{i,k} \cdot \frac{k}{m} , \quad (18)$$

$$\zeta_i = \lambda_{i,k-1} \cdot \frac{(k-1)^2}{m^2} + \lambda_{i,k} \cdot \frac{k^2}{m^2} , \quad (19)$$

where $\lambda_{i,k-1}$ and $\lambda_{i,k}$ are two weights and satisfy the following constraints.

$$\lambda_{i,k-1} + \lambda_{i,k} = 1 , \quad (20)$$

$$0 \leq \lambda_{i,k-1}, \lambda_{i,k} \leq 1 . \quad (21)$$

Since $y = x^2$ is a convex function, the piecewise linear approximation curve (η_i, ζ_i) lies above the curve (η_i, η_i^2), $0 \leq \eta_i \leq 1$. Thus, we have $\zeta_i \geq \eta_i^2$ (see Fig. 3). The following lemma characterizes the approximation error $\zeta_i - \eta_i^2$ as a function of m. Its proof can be found in [16].

Lemma 3: $\zeta_i - \eta_i^2 \leq \frac{1}{4m^2}$ for $i \in \mathcal{N}$.

Note that the mathematical representation in (18) to (21) is for a given kth segment, $k = 1, 2, \cdots, m$. We now give a

mathematical formulation for the entire piecewise linear curve. Denote z_{ik}, $1 \le k \le m$, a binary variable indicating whether η_i falls within the kth segment, i.e., if $\frac{k-1}{m} \le \eta_i < \frac{k}{m}$, then $z_{ik} = 1$, otherwise, $z_{ik} = 0$. Since η_i can only fall in one of the m segments, we have

$$\sum_{k=1}^{m} z_{ik} = 1 . \tag{22}$$

With the definition of z_{ik}, $1 \le k \le m$, we can formulate (18) to (20) for the entire piecewise linear curve. First, we show how λ_{ik} relates to z_{ik}, $1 \le k \le m$. Based on (18) to (20), when η_i falls in the kth segment, we can only have $\lambda_{i,k-1}$ and $\lambda_{i,k}$ be positive while all other $\lambda_{i,j}$ ($j \ne k-1, k$) be all zero. That is, $\lambda_{i0} > 0$ only if $z_{i1} = 1$; $\lambda_{ik} > 0$ only if $z_{ik} = 1$ or $z_{i,k+1} = 1$, $1 \le k < m$; and $\lambda_{im} > 0$ only if $z_{im} = 1$. These relationships can be written as follows.

$$\lambda_{i0} \le z_{i1} \tag{23}$$
$$\lambda_{ik} \le z_{ik} + z_{i,k+1} \quad (1 \le k < m) \tag{24}$$
$$\lambda_{im} \le z_{im} \tag{25}$$

The above three constraints ensure that there are at most two adjacent positive λ's for each η_i, (18), (19), and (20) can now be rewritten for the entire piecewise linear curve as follows.

$$\eta_i = \sum_{k=0}^{m} \lambda_{ik} \cdot \frac{k}{m} \tag{26}$$
$$\zeta_i = \sum_{k=0}^{m} \lambda_{ik} \cdot \frac{k^2}{m^2} \tag{27}$$
$$\sum_{k=0}^{m} \lambda_{ik} = 1 \tag{28}$$

Relaxed Linear Formulation. By replacing η_i^2 with ζ_i in (17), we have

$$\eta_{\text{vac}} \le 1 - \sum_{k \in \mathcal{N}} \eta_k - \frac{U \tau_{\text{TSP}}}{E_{\max} - E_{\min}}(\eta_i - \zeta_i) \quad (i \in \mathcal{N}). \tag{29}$$

By adding new constraints (22) to (28), we have the following linear relaxed formulation.

OPT-L

$$\begin{aligned}
\max \quad & \eta_{\text{vac}} \\
s.t. \quad & (15), (16), (22) - (29) \\
& f_{ij}, f_{iB} \ge 0, 0 \le \eta_i, \eta_{\text{vac}}, \zeta_i \le 1 \quad (i, j \in \mathcal{N}, i \ne j) \\
& z_{ik} \in \{0, 1\} \quad (i \in \mathcal{N}, 1 \le k \le m) \\
& 0 \le \lambda_{ik} \le 1 \quad (i \in \mathcal{N}, 0 \le k \le m),
\end{aligned}$$

where f_{ij}, f_{iB}, η_i, η_{vac}, z_{ik}, λ_{ik}, and ζ_i are variables, R_i, C, C_{ij}, C_{iB}, U, $E_{\max}$, $E_{\min}$, and τ_{TSP} are constants. The new formulation can now be solved by a solver such as CPLEX [19].

Construction of Feasible Near-Optimal Solution. The solution to problem OPT-L is likely to be infeasible to problem OPT-R (and problem OPT). But based on this solution, we can construct a feasible solution to problem OPT.

Suppose $\hat{\psi} = (\hat{f}_{ij}, \hat{f}_{iB}, \hat{\eta}_i, \hat{\eta}_{\text{vac}}, \hat{z}_{ik}, \hat{\lambda}_{ik}, \hat{\zeta}_i)$ is the solution to problem OPT-L. Looking at $(\hat{f}_{ij}, \hat{f}_{iB}, \hat{\eta}_i, \hat{\eta}_{\text{vac}})$, we find that it satisfies all constraints to problem OPT-R except (17). To construct a feasible solution $\psi = (f_{ij}, f_{iB}, \eta_i, \eta_{\text{vac}})$ to problem OPT-R, we let $f_{ij} = \hat{f}_{ij}$, $f_{iB} = \hat{f}_{iB}$, $\eta_i = \hat{\eta}_i$. For η_{vac}, in order to satisfy (17), we define it as

$$\eta_{\text{vac}} = \min_{i \in \mathcal{N}} \left\{ 1 - \sum_{k \in \mathcal{N}} \hat{\eta}_k - \frac{U \cdot \tau_{\text{TSP}}}{E_{\max} - E_{\min}} \hat{\eta}_i (1 - \hat{\eta}_i) \right\} .$$

It is easy to verify that this newly constructed solution ψ satisfies all constraints for problem OPT-R. Once we have this solution to problem OPT-R, we can easily find a solution to problem OPT via Algorithm 1.

D. Proof of Near-Optimality

In this section, we quantify the performance gap between the optimal objective (unknown, denoted as η_{vac}^*) and the objective (denoted as η_{vac}) obtained by the feasible solution ψ that we obtained in the last section. Naturally, we expect such performance gap is a function of m, i.e., the number of segments that we use in the piecewise linear approximation. This result will be stated in Lemma 4. Based on this result, we can obtain an important inverse result (in Theorem 2), which shows that for a given target performance gap ϵ ($0 < \epsilon \ll 1$), how to set m such that $\eta_{\text{vac}}^* - \eta_{\text{vac}} \le \epsilon$.

Lemma 4: For the feasible solution ψ with objective value η_{vac}, we have $\eta_{\text{vac}}^* - \eta_{\text{vac}} \le \frac{U \cdot \tau_{\text{TSP}}}{4(E_{\max} - E_{\min})} \cdot \frac{1}{m^2}$.

Proof: Denote $\hat{\eta}_{\text{vac}}$ the objective value obtained by solution $\hat{\psi}$ to the relaxed linear problem OPT-L. Since problem OPT-L is a relaxation of problem OPT-R, $\hat{\eta}_{\text{vac}}$ is an upper bound of η_{vac}^*, i.e., $\eta_{\text{vac}}^* \le \hat{\eta}_{\text{vac}}$. Therefore,

$$\begin{aligned}
& \eta_{\text{vac}}^* - \eta_{\text{vac}} \\
\le \quad & \hat{\eta}_{\text{vac}} - \eta_{\text{vac}} \\
= \quad & \left[1 - \sum_{k \in \mathcal{N}} \hat{\eta}_k - \frac{U \tau_{\text{TSP}}}{E_{\max} - E_{\min}} \cdot (\eta_{\max} - \zeta_{\max}) \right] \\
& - \left[1 - \sum_{k \in \mathcal{N}} \hat{\eta}_k - \frac{U \tau_{\text{TSP}}}{E_{\max} - E_{\min}} \cdot \eta_{\max} \cdot (1 - \eta_{\max}) \right] \\
= \quad & \frac{U \tau_{\text{TSP}}}{E_{\max} - E_{\min}} (\zeta_{\max} - \eta_{\max}^2) \\
\le \quad & \frac{U \tau_{\text{TSP}}}{4(E_{\max} - E_{\min})} \cdot \frac{1}{m^2},
\end{aligned}$$

where the second equality holds by Lemmas 5 and 6 in [16], the fourth inequality holds by Lemma 3. This completes the proof. ∎

Based on Lemma 4, the following theorem shows that for a given target performance gap ϵ ($0 < \epsilon \ll 1$), how to set m such that $\eta_{\text{vac}}^* - \eta_{\text{vac}} \le \epsilon$.

Theorem 2: For a given ϵ, $0 < \epsilon \ll 1$, if $m = \left\lceil \sqrt{\frac{U \tau_{\text{TSP}}}{4\epsilon(E_{\max} - E_{\min})}} \right\rceil$, then we have $\eta_{\text{vac}}^* - \eta_{\text{vac}} \le \epsilon$.

Proof: Lemma 4 shows that the performance gap is $\eta_{\text{vac}}^* - \eta_{\text{vac}} \le \frac{U \tau_{\text{TSP}}}{4(E_{\max} - E_{\min})} \cdot \frac{1}{m^2}$. Therefore, if we set $m = \left\lceil \sqrt{\frac{U \tau_{\text{TSP}}}{4\epsilon(E_{\max} - E_{\min})}} \right\rceil \ge \sqrt{\frac{U \tau_{\text{TSP}}}{4\epsilon(E_{\max} - E_{\min})}}$, then we have

$$\begin{aligned}
\eta_{\text{vac}}^* - \eta_{\text{vac}} \quad \le \quad & \frac{U \tau_{\text{TSP}}}{4(E_{\max} - E_{\min})} \cdot \frac{1}{m^2} \\
\le \quad & \frac{U \tau_{\text{TSP}}}{4(E_{\max} - E_{\min})} \cdot \frac{4\epsilon(E_{\max} - E_{\min})}{U \tau_{\text{TSP}}} \\
= \quad & \epsilon .
\end{aligned}$$

This completes the proof. ∎

With Theorem 2, we show the complete solution procedure on how to obtain a near-optimal solution to OPT in Fig. 4.

Fig. 4. Summary of the construction of a near-optimal solution.

Fig. 5. Illustration of energy behavior for the initial transient cycle and how it connects the first renewable cycle.

VII. CONSTRUCTION OF INITIAL TRANSIENT CYCLE

In Section IV, we skipped discussion on how to construct the initial transient cycle before the first renewable cycle. Now with the optimal traveling path P (the shortest Hamiltonian cycle) and the feasible near-optimal solution $(f_{ij}, f_{iB}, \tau, \tau_i, \tau_{\mathrm{vac}}, p_i)$ obtained in Section VI, we are ready to construct the initial transient cycle.

Unlike a renewable energy cycle at node i, which starts and ends with the same energy level E_i, the initial transient starts with $E_{\max}$ and ends with E_i. Specifically, the initial transient cycle must meet the following criterion.

Criterion 1: At each node $i \in \mathcal{N}$, its initial transient cycle must meet the following criteria: (i) $e_i(0) = E_{\max}$ and $e_i(\tau) = E_i$; and (ii) $e_i(t) \geq E_{\min}$ for $t \in [0, \tau]$.

We now construct an initial cycle to meet the above criterion. First, we need to calculate E_i ($i \in \mathcal{N}$). From (6), we have $E_i = E_{\max} - (2\tau - a_i - \tau_i)p_i$, where a_i can be obtained by (3).

For a solution $\varphi = (P, f_{ij}, f_{iB}, \tau, \tau_i, \tau_P, \tau_{\mathrm{vac}}, p_i, U)$ corresponding to a renewable energy cycle for $t \geq \tau$, we construct $\hat{\varphi} = (\hat{P}, \hat{f}_{ij}, \hat{f}_{iB}, \hat{\tau}, \hat{\tau}_i, \hat{\tau}_{\hat{P}}, \hat{\tau}_{\mathrm{vac}}, \hat{p}_i, u_i)$ for the initial transient cycle for $t \in [0, \tau]$ by letting $\hat{P} = P$, $\hat{f}_{ij} = f_{ij}$, $\hat{f}_{iB} = f_{iB}$, $\hat{\tau} = \tau$, $\hat{\tau}_i = \tau_i$, $\hat{\tau}_{\hat{P}} = \tau_P$, $\hat{\tau}_{\mathrm{vac}} = \tau_{\mathrm{vac}}$, $\hat{p}_i = p_i$ and

$$u_i = \frac{p_i \hat{a}_i}{\tau_i} + p_i, \qquad (30)$$

where u_i is the charging rate at node i during the initial transient cycle and $\hat{a}_i$ is the arrival time of the WCV at node i in the initial transient cycle (see Fig. 5).

Now we need to show $u_i \leq U$ where U is the full charging rate. First we have

$$
\begin{aligned}
\hat{a}_{\pi_i} &= \sum_{k=0}^{i-1} \frac{\hat{D}_{\pi_k \pi_{k+1}}}{V} + \sum_{k=1}^{i-1} \hat{\tau}_k \\
&= \sum_{k=0}^{i-1} \frac{D_{\pi_k \pi_{k+1}}}{V} + \sum_{k=1}^{i-1} \tau_k = a_{\pi_i} - \tau , \qquad (31)
\end{aligned}
$$

where the second equality holds by $\hat{P} = P$ and $\hat{\tau}_i = \tau_i$, and the last equality follows from (3). Further, by (5), we have $U \cdot \tau_i = \tau \cdot p_i = (2\tau - \tau) \cdot p_i \geq (a_i + \tau_i - \tau) \cdot p_i$. It follows that

$$(a_i - \tau) \cdot p_i \leq (U - p_i) \cdot \tau_i. \qquad (32)$$

Then, we have

$$
\begin{aligned}
u_i &= \frac{p_i \hat{a}_i}{\tau_i} + p_i = \frac{p_i(a_i - \tau)}{\tau_i} + p_i \\
&\leq \frac{(U - p_i) \cdot \tau_i}{\tau_i} + p_i = U ,
\end{aligned}
$$

where the first equality follows from (30), the second equality follows from (31), and the third inequality follows from (32).

For the newly constructed $\hat{\varphi}$, we have the following theorem.

Theorem 3: The constructed $\hat{\varphi}$ is a feasible transient cycle.

To prove $\hat{\varphi}$ is a feasible initial transient cycle, we need to show that the newly constructed $\hat{\varphi}$ satisfies Criterion 1, which can be easily proved [16].

VIII. NUMERICAL RESULTS

In this section, we present some numerical results to demonstrate how our solution can produce a renewable WSN and some interesting properties with such a network.

A. Simulation Settings

We consider a randomly generated WSN consisting of 50 nodes. [2] The sensor nodes are deployed over a square area of 1 km × 1 km. The data rate (i.e., R_i, $i \in \mathcal{N}$) from each node is randomly generated within $[1, 10]$ kb/s. The power consumption coefficients are $\beta_1 = 50$ nJ/b, $\beta_2 = 0.0013$ pJ/(b · m^4), $\alpha = 4$, and $\rho = 50$ nJ/b [20]. The base station is assumed to be located at $(500, 500)$ (in m) and the home service station for the WCV is assumed to be at the origin. The traveling speed of the WCV is $V = 5$ m/s.

For the battery at a sensor node, we choose a regular NiMH battery and its nominal cell voltage and the quantity of electricity is 1.2 V/2.5 Ah. We have $E_{\max} = 1.2$ V × 2.5 A × 3600 sec = 10.8 KJ [21, Chapter 1]. We let $E_{\min} = 0.05 \cdot E_{\max} = 540$ J. We assume the wireless energy transfer rate $U = 5$ W, which is well within feasible range [11].

We set the target $\epsilon = 0.01$ for the numerical results, i.e., our solution is within 1% from the optimum.

B. Results

Table I gives the location of each node and its data rate for a 50-node network. The shortest Hamiltonian cycle is found by using the Concorde solver [18] and is shown in Fig. 6. For

---

[2]Additional results for other network sizes can be found in [16].

TABLE I
LOCATION AND DATA RATE R_i FOR EACH NODE IN A 50-NODE NETWORK.

Node Index	Location (m)	R_i (kb/s)	Node Index	Location (m)	R_i (kb/s)
1	(815, 276)	2	26	(758, 350)	9
2	(906, 680)	8	27	(743, 197)	1
3	(127, 655)	4	28	(392, 251)	4
4	(913, 163)	6	29	(655, 616)	3
5	(632, 119)	2	30	(171, 473)	9
6	(98, 498)	7	31	(706, 352)	5
7	(278, 960)	3	32	(32, 831)	10
8	(547, 340)	7	33	(277, 585)	2
9	(958, 585)	7	34	(46, 550)	3
10	(965, 224)	8	35	(97, 917)	2
11	(158, 751)	5	36	(823, 286)	2
12	(971, 255)	1	37	(695, 757)	9
13	(957, 506)	3	38	(317, 754)	6
14	(485, 699)	10	39	(950, 380)	6
15	(800, 891)	2	40	(34, 568)	2
16	(142, 959)	9	41	(439, 76)	9
17	(422, 547)	6	42	(382, 54)	7
18	(916, 139)	10	43	(766, 531)	4
19	(792, 149)	1	44	(795, 779)	6
20	(959, 258)	5	45	(187, 934)	5
21	(656, 841)	2	46	(490, 130)	1
22	(36, 254)	10	47	(446, 569)	3
23	(849, 814)	1	48	(646, 469)	2
24	(934, 244)	8	49	(709, 12)	2
25	(679, 929)	9	50	(755, 337)	3
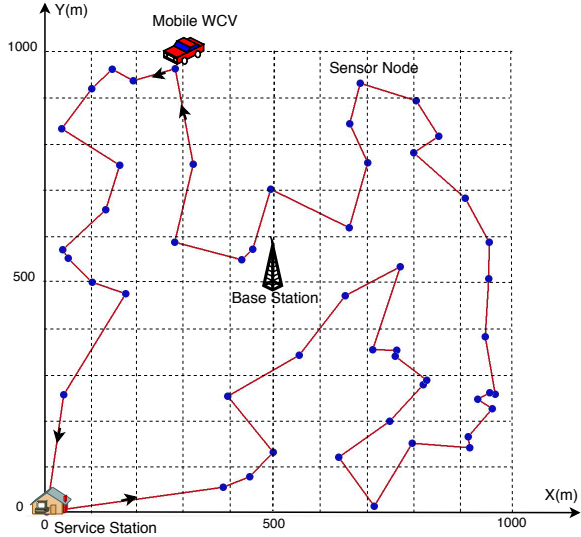
Fig. 6. An optimal traveling path for the 50-node sensor network. Only counter clockwise traveling direction is shown.

this optimal cycle, $D_{\mathrm{TSP}} = 5821$ m and $\tau_{\mathrm{TSP}} = 1164.2$ s. For the target $\epsilon = 0.01$, by Theorem 2, we have

$$m = \left\lceil \sqrt{\frac{U \cdot \tau_{\mathrm{TSP}}}{4\epsilon (E_{\max} - E_{\min})}} \right\rceil$$
$$= \left\lceil \sqrt{\frac{5 \times 1164.2}{4 \times 0.01 \times (10800 - 540)}} \right\rceil = 4 \,,$$

which is a small number. In our solution, we have the cycle time $\tau = 17.34$ hours, the vacation time $\tau_{\mathrm{vac}} = 13.44$ hours, and the objective $\eta_{\mathrm{vac}} = 77.51\%$.

In Corollary 1.2, we find that the WCV can follow either direction of the shortest Hamiltonian cycle while achieving
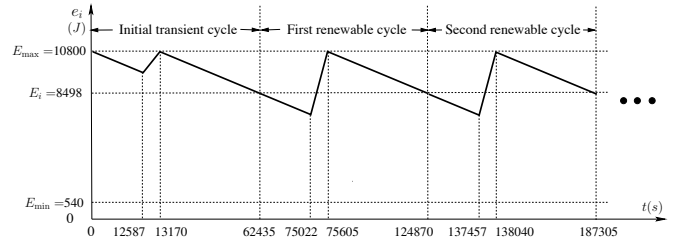
(a) Traveling path is counter clockwise.
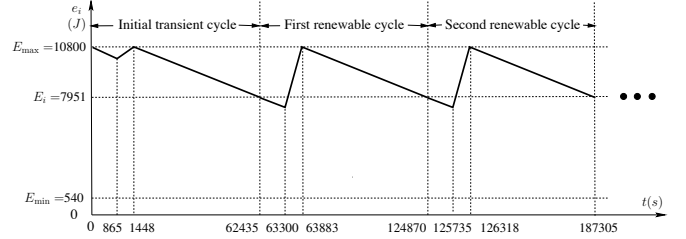
(b) Traveling path is clockwise.

Fig. 7. The energy behavior of a sensor node (the 6th) in the 50-node network during the initial transient cycle and the first two renewable cycles.
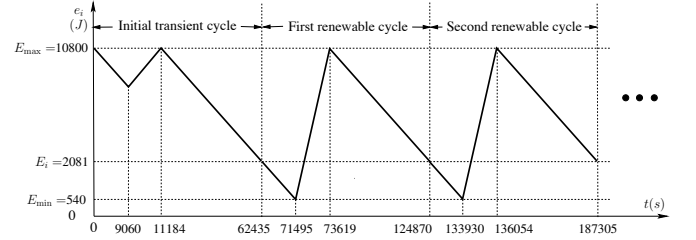
Fig. 8. The energy behavior of the bottleneck node (38th node) in the 50-node network. Traveling direction is counter clockwise.

the same objective value $\eta_{\mathrm{vac}} = 77.51\%$. Comparing the two solutions, the values for f_{ij}, f_{iB}, τ, τ_i, τ_{TSP}, τ_{vac} are identical while the values of a_i and E_i are different. This finding can be verified by our numerical results. As an example, Figs. 7(a) and 7(b) show the energy cycle behavior of a sensor node (the 6th node) under the two opposite traveling directions, respectively.

In Property 1, we find that there exists a bottleneck node in the network with its energy dropping to $E_{\min}$ during a renewable energy cycle. This property is confirmed in our numerical results. This bottleneck node is the 38th node, whose energy behavior is shown in Fig. 8.

In Section VI-B, we showed that minimum energy routing may not be optimal for our problem (see Remark 1). This point is confirmed by our numerical results. In Fig. 9, we show that data routing in our solution differs from the minimum energy routing.

IX. CONCLUSION

Existing WSN is constrained by limited battery energy at a node and thus finite lifetime is regarded as a fundamental performance bottleneck. This paper exploits recent breakthrough in wireless energy transfer technology for a WSN and shows that once properly designed, a WSN has the potential to

(a) Data routing in our solution. (b) Minimum energy routing.
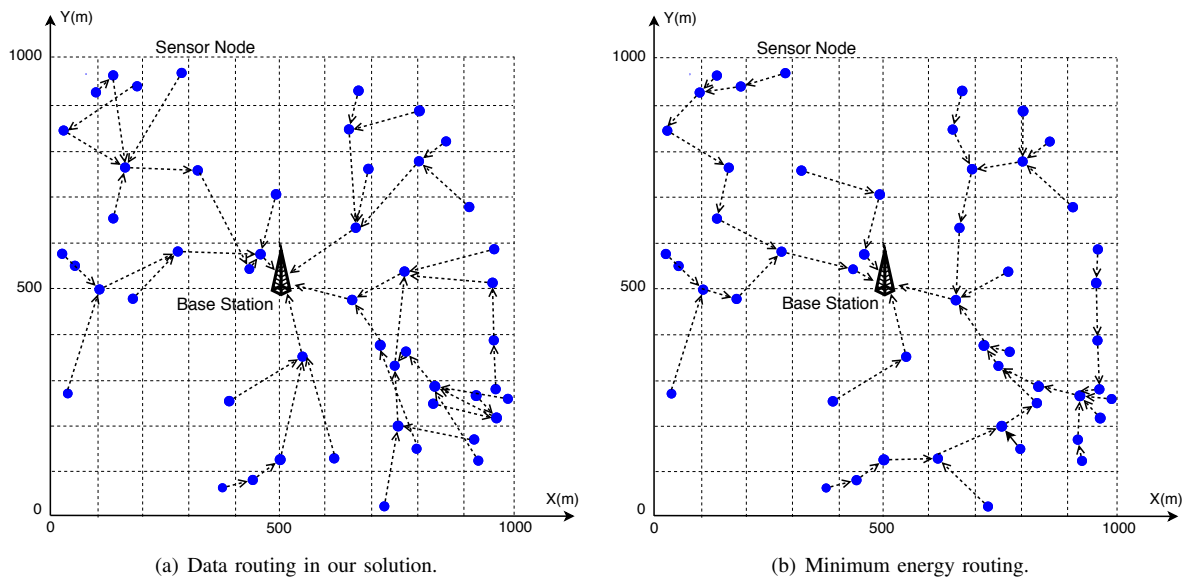
Fig. 9. Comparison of data routing by our solution and that by minimum energy routing for the 50-node network.

remain operational forever. This is the first paper that offers a systematic investigation of a sensor network operation under this new enabling energy transfer technology.

We studied a general scenario where a mobile charging vehicle periodically travels inside the network and charges each sensor node wirelessly without any plugs or wires. We introduced a new concept called renewable energy cycle and offered both necessary and sufficient conditions. We studied a practical optimization problem, with the objective of maximizing the ratio of the WCV's vacation time over the cycle time. For this problem, we proved that the optimal traveling path for the WCV in each renewable cycle is the shortest Hamiltonian cycle. Subsequently, we developed a provable near-optimal solution for both flow routing, total cycle time, and individual charging time at each node. We also showed that traditional minimum energy routing cannot achieve optimal solution. Using numerical results, we showed the detailed network behavior within a renewable energy cycle and demonstrated that a sensor network operating under our solution can indeed remain operational with unlimited lifetime.

REFERENCES

[1] J. Chang and L. Tassiulas, "Maximum lifetime routing in wireless sensor networks," *IEEE/ACM Trans. on Networking,* vol. 12, no. 4, pp. 609–619, Aug. 2004.

[2] W. Wang, V. Srinivasan, and K.C. Chua, "Using mobile relays to prolong the lifetime of wireless sensor networks," in *Proc. ACM MobiCom,* Cologne, Germany, Aug. 2005, pp. 270–283.

[3] A. Giridhar and P.R. Kumar, "Maximizing the functional lifetime of sensor networks," in *Proc. ACM/IEEE International Symposium on Information Processing in Sensor Networks,* Los Angeles, CA, Apr. 2005, pp. 5–12.

[4] Y.T. Hou, Y. Shi, and H.D. Sherali, "Rate allocation and network lifetime problems for wireless sensor networks," *IEEE/ACM Trans. on Networking,* vol. 16, no. 2, pp. 321–334, Apr. 2008.

[5] Y. Shi and Y.T. Hou, "Theoretical results on base station movement problem for sensor network," in *Proc. IEEE INFOCOM,* Phoenix, AZ, Apr. 2008, pp. 376–384.

[6] X. Jiang, J. Polastre, and D. Culler, "Perpetual environmentally powered sensor networks," in *Proc. ACM/IEEE International Symposium on Information Processing in Sensor Networks,* Los Angeles, CA, Apr. 2005, pp. 463–468.

[7] A. Kansal, J. Hsu, S. Zahedi, and M.B. Srivastava, "Power management in energy harvesting sensor networks," *ACM Trans. Embed. Comput. Syst.,* vol. 6, no. 4, article 32, Sep. 2007.

[8] N. Bulusu and S. Jha (eds.), *Wireless Sensor Networks: A Systems Perspective,* Norwood, MA: Artech House, 2005.

[9] Y. Ammar, A. Buhrig, M. Marzencki, B. Charlot, S. Basrour, K. Matou, and M. Renaudin, "Wireless sensor network node with asynchronous architecture and vibration harvesting micro power generator," in *Proc. of Joint Conference on Smart Objects and Ambient Intelligence: Innovative Context-Aware Services: Usages and Technologies,* Grenoble, France, Oct. 12–14, 2005, pp. 287–292.

[10] G. Park, T. Rosing, M.D. Todd, C.R. Farrar, and W. Hodgkiss, "Energy harvesting for structural health monitoring sensor networks," *J. Infrastruct. Syst.,* vol. 14, no. 1, pp. 64–79, Mar. 2008.

[11] A. Kurs, A. Karalis, R. Moffatt, J.D. Joannopoulos, P. Fisher, and M. Soljacic, "Wireless power transfer via strongly coupled magnetic resonances," *Science,* vol. 317, no. 5834, pp. 83–86, 2007.

[12] F. Zhang, X. Liu, S.A. Hackworth, R.J. Sclabassi, and M. Sun, "In vitro and in vivo studies on wireless powering of medical sensors and implantable devices," in *Proc. IEEE/NIH Life Science Systems and Applications Workshop (LiSSA),* pp. 84–87, Apr. 2009, Bethesda, MD.

[13] N. Tesla, "Apparatus for transmitting electrical energy," US patent number 1,119,732, issued in Dec. 1914.

[14] T.A. Vanderelli, J.G. Shearer, and J.R. Shearer, "Method and apparatus for a wireless power supply," U.S. patent number 7,027,311, issued in Apr. 2006.

[15] Wireless Power Consortium, http://www.wirelesspowerconsortium.com/.

[16] Y. Shi, L. Xie, Y.T. Hou, and H.D. Sherali, "On renewable sensor networks with wireless energy transfer," Technical Report, the Bradley Department of Electrical and Computer Engineering, Virginia Tech, Blacksburg, VA, July 2010. Available at http://filebox.vt.edu/users/yshi/papers/charging.pdf.

[17] M. Padberg and G. Rinaldi, "A branch-and-cut algorithm for the resolution of large-scale symmetric traveling salesman problems," *SIAM Review,* vol. 33, no. 1, pp. 60–100, 1991.

[18] Concorde TSP Solver, http://www.tsp.gatech.edu/concorde/.

[19] IBM ILOG CPLEX Optimizer, http://www-01.ibm.com/software/integration/optimization/cplex-optimizer/.

[20] W. Heinzklman, "Application-specific protocol architectures for wilress networks," *Ph.D. dessertation,* Dept. Elect. Eng. Comput. Sci., MIT, Cambridge, MA, Jun. 2000.

[21] D. Linden and T.B. Reddy (eds.), *Handbook of Batteries,* Third Edition, McGraw-Hill, 2002.